DTU Library

Model-based analysis and optimization of a full-scale industrial high-rate anaerobic bioreactor

Feldman, H.; Flores-Alsina, X.; Kjellberg, K.; Jeppsson, U.; Batstone, D. J.; Gernaey, K. V.

Published in:
Biotechnology and Bioengineering

Link to article, DOI:
10.1002/bit.26807

Publication date:
2018

Document Version
Peer reviewed version

Hannah Feldman ORCID iD: 0000-0001-7314-3094

Model-based analysis and optimization of a full-scale industrial high-rate anaerobic bioreactor

H. Feldman[1*], X. Flores-Alsina[1], K. Kjellberg[2], U. Jeppsson[3], D.J. Batstone[4], K.V. Gernaey[1]

[1] Process and Systems Engineering Center (PROSYS), Department of Chemical and Biochemical Engineering, Technical University of Denmark, Building 229, DK-2800 Kgs. Lyngby, Denmark.

[2] Novozymes A/S, Hallas Alle 1, DK-4400 Kalundborg, Denmark.

[3] Division of Industrial Electrical Engineering and Automation, Department of Biomedical Engineering, Lund University, Box 118, SE-221 00 Lund, Sweden.

[4] Advanced Water Management Centre, The University of Queensland, St Lucia, Brisbane, Queensland 4072 Australia.

[*]Corresponding author: hafe@kt.dtu.dk; +45 45252811

Running title: Modelling of a full-scale anaerobic reactor

RESEARCH HIGHLIGHTS

- An industrial high-rate anaerobic bioreactor model is constructed
- Influent fractionation is based on COD, N, P and S balances
- The model describes two full-scale data sets with average deviations of 13 % and 15 %

This article has been accepted for publication and undergone full peer review but has not been through the copyediting, typesetting, pagination and proofreading process, which may lead to differences between this version and the Version of Record. Please cite this article as doi: 10.1002/bit.26807.

- Response surfaces indicate optimal operational conditions are highly dependent on operational pH
- Optimization results reveal a low impact of S removal and CO_2 stripping on energy recovery, while an impact on the caustic addition was observed for both strategies.

ABSTRACT

The objective of this paper is to present the model-based optimization results of an anaerobic granular sludge internal circulation (IC) reactor. The International Water Association (IWA) Anaerobic Digestion Model No. 1 extended with phosphorus (P), sulphur (S) and ethanol (Et-OH) is used to describe the main biological and physico-chemical processes. The high-rate conditions within the reactor are simulated using a flow + reactor model comprised of a series of continuous stirred tank reactors (CSTRs) followed by an ideal total suspended solids (TSS) separation unit. Following parameter estimation by least squares on the measured data, the model had a relative mean error of 13 % and 15 % for Dataset #1 and Dataset #2, respectively. Response surfaces (RSs) show that the reactor performance index (RPI) (a metric combining energy recovery in the form of heat and electricity, as well as chemicals needed for pH control) could be improved by 45 % when reactor pH is reduced down to 6.8. Model-based results reveal that influent S does not impose sufficient negative impacts on energy recovery (+ 5.7 %, in MWh/day, + 0.20 M€/year when influent S is removed) to warrant the cost of its removal (3.58 M€/year). In fact, the process could handle even higher S loads (ensuring the same degree of conversion) as long as the pH is maintained above 6.8. Nevertheless, a higher S load substantially increases the amount of added *NaOH* to maintain the desired operational pH (> 25 %) due to the acidic behaviour of HS^-. CO_2 stripping

decreases the buffer capacity of the system and hence use of chemicals for pH control. Finally, the paper discusses possibilities and limitations of the proposed approach, and how the results of this study will be put into practice.

Graphical Abstract

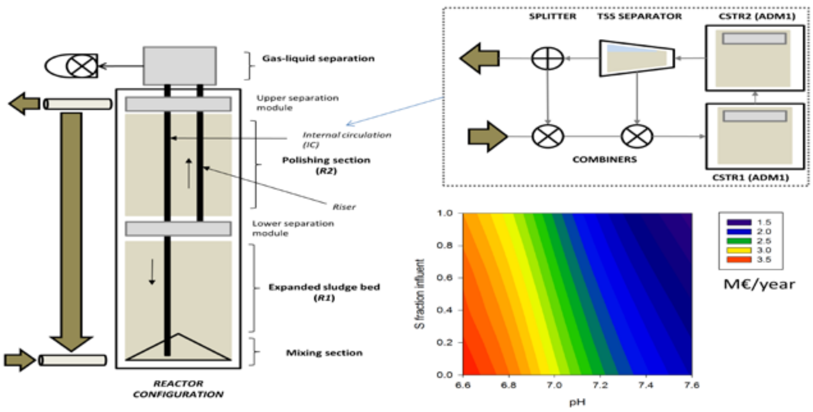

The objective of this paper is to present the model-based optimization results of an anaerobic granular sludge internal circulation (IC) reactor.

KEYWORDS

ADM1, benchmarking, energy recovery, high-rate reactors, sulfide production, response surfaces

1. INTRODUCTION

Industrial wastewaters have special characteristics (compared to urban wastewater), which are a result of the specific function of the upstream factory (**Sipma et al., 2010**). Variable pH (**Fang and Liu, 2002**), influent biodegradability (**Astals et al., 2013**) and non-standard N:COD and P:COD ratios (**Punal et al., 2000**) challenge traditional biological processes. In some cases, high sulfur (S) loads can dramatically decrease methane/biogas production (and potential energy recovery) (**Metcalf & Eddy et al., 2003**). This reduction is attributed to two factors: 1) loss of electron equivalents due to sulfate reducing bacteria (**Hao et al., 2014; Yun et al., 2017**); and, 2) inhibition of acetoclastic and hydrogenotrophic methanogenesis due to sulfide inhibition (**Kalyuzhnyi and Fedorovich, 1998**). Metals and some inorganic/organic compounds can also inhibit microorganism growth and/or have severe toxicity effects (**Chen et al., 2008**). The high content of cations and anions promotes the formation of precipitates at different locations in the reactor (granules, pipes), which can have detrimental (decrease of methanogenic activity) or catastrophic (cementation) effects on reactor performance (**Van Langerak et al., 1998; 2000**). Hence, mathematical (process) models describing industrial wastewater reactors should include all these (hostile) phenomena in order to provide functional representation of full-scale processes.

The field of systems analysis in wastewater engineering has been rapidly expanding, including specific anaerobic digestion (AD) models, such as the IWA Anaerobic Digestion Model No. 1 (ADM1) (**Batstone et al., 2002a**). Numerous studies presenting (mathematical) approaches describing new technologies, new processes and the need to consider anaerobic systems in a much broader context of the wastewater cycle as a whole have been published in specialized literature (**Batstone et al., 2015**). Within the area of new technologies, there is an increasing interest, particularly for industrial applications, to develop models for sludge bed systems containing biofilms, such as anaerobic contact processes (ACP), anaerobic filters (AF), up-flow anaerobic sludge blanket (UASB) reactors, fluidized bed (FB) reactors, expanded granular sludge bed (ESGB) reactors and internal recirculation (IC) reactors (**van Lier et al., 2015**).

Other important factors to account for when representing sludge bed systems are flow and reactor models (**Saravanan and Sreekrishnan, 2006**). With respect to flow patterns there are numerous studies in literature proposing several hydraulic schemes (**Batstone et al., 2005; Bolle et al., 1986; Chen et al., 2009**). Indeed, the flow model should be able to describe the dynamics of particulates for example, in the sludge bed, the sludge blanket and the polishing section as well as the effect of multiple splitters/combiners (**Ren et al., 2009**). Regarding reactor models, it is important to reproduce high-rate conditions representing biomass accumulation. In these situations, granular type models could be implemented since they account for mass transfer limitations and microbial competition/affinity within the biofilm (**Wanner et al., 2006**). The works of **Batstone et al. (2004)**, **Odriozola et al. (2016)** and **Feldman et al. (2017)** show the benefits of using multi-scale models (biofilm, granule, reactor) when predicting process performance, microbial community structure and how these interact, and how they are affected by changing loading conditions.

High rate conditions can also be empirically represented by artificially separating the hydraulic and the sludge retention time (**Batstone et al., 2002b; Vanhooren et al., 2002**), without the need of overcomplicated biofilm reactors. Indeed, it is well known that the multi-scale (spatial/temporal) nature of biofilm/granular models (**Xavier et al., 2005**) makes them very unstable (difficult to reach steady state), stiff (computationally demanding) and consequently very difficult to calibrate (**Boltz et al., 2010; Brockmann et al., 2013**). This might pose a major problem, particularly within an industrial context, where the time horizon for obtaining results is often relatively short, which conflicts with the fact that many simulations might be required to determine optimal operational conditions (**Rieger et al., 2012**).

The main objective of this paper is to present the model-based implementation of a full-scale anaerobic granular IC reactor treating industrial wastewater from the fermentation industry producing various pharmaceutical and enzymatic products (depending on production schedule), and to use this model for optimization of the operational conditions to improve reactor performance. Typical high-rate conditions are reproduced using a flow + reactor model comprised of a series of continuous stirred tank reactors (CSTRs) followed by an ideal total suspended solids (TSS) separation unit. Biological and physico-chemical processes are based on the ADM1 upgraded with the fate of P and S compounds, the role of ethanol as well as an improved physico-chemical description in order to correctly deal with wastewater produced in industry. The study is sub-divided into three parts:

(1) Influent fractionation based on rigorous COD, N, P and S balances to correctly characterize biodegradability from available measurements;
(2) Model development, parameter adjustment and model verification using two different data sets corresponding to different operational periods;
(3) Creation of response surfaces (*RSs*) to identify the best strategy to maximize energy (electricity/heat) recovery and minimize operational costs.

2. METHODS

2.1 Plant configuration

The plant under study is a BIOPAQ®IC reactor (Paques, the Netherlands) and is comprised of four sections, with a total liquid volume (V_{liq}) of 1963 m^3 and gas volume (V_{gas}) of 213 m^3: i) mixing section (*M*); ii) expanded sludge bed (*R1*); iii) polishing section (*R2*); and, iv) gas liquid separator (*G – L*). In *M* the influent is evenly distributed within the reactor. The water flows upwards to *R1* where most of the organics are converted into biogas. Next, the biogas produced is collected in the lower separation module and flows upwards through the riser to *G – L* at the top of the reactor. In this section the water and biogas are separated. A fraction of the water flows down into the downer to the bottom and is mixed with the influent. This fraction is internally controlled based on the gas production, i.e. the more gas produced, the more water flows downwards. The flow of water from *R1* through the riser and the downer and back into *M* is called internal circulation (IC) and it gives the reactor its name. The water from *R1* flows to the upper compartment (*R*2), which is lower on organic material. In this section the rest of the biodegradable organic material is transformed into biogas. This biogas flows upwards to *G – L*. Again biogas is separated in this section, while water is sent to *M* through the downer. The biogas leaves the reactor at the top and the polished effluent through the effluent pipe (see **Figure 1** for details). The effluent is led to a recirculation tank (*RT*), where a fraction of the effluent is mixed with influent wastewater. This increases the flow rate to the IC reactor from 3 460 m^3/d to 12 720 m^3/d, without increasing the loading of organic compounds to the reactor.

2.2. Data collection and influent generation

Two (#*D*1 and #*D*2) different data sets corresponding to two operational periods (25.01.2016 to 11.02.2016 and 28.08.2016 to 19.09.2016, respectively) are used to test the predictive capabilities of the model. Daily measurements of the influent and effluent are available of nutrients (N, P), COD, different types of S forms (SO_4^{-2}, H_2S) and minerals and ions (Na^+, K^+, Ca^{2+}, Mg^{2+}, Cl^-), as well as continuous measurements of pH, flow rate, VFA and alkalinity. Furthermore, gas flow rate and fractions (CH_4 and CO_2) are available from continuous monitoring of the gas composition and energy production. H_2S fractions are measured daily. Analyses are done using Standard Methods (**APHA et al., 2012**).

It is important to highlight that influent conditions are extremely variable since the system under investigation treats the wastewater of two major biotechnology industries (Novozymes, Novo-Nordisk) located in the NW part of Zealand, Denmark (see averages in **Table S1** for #*D*1 and #*D*2). Indeed, wastewater quality/quantity strongly depends on production schedules, which change over the year. Furthermore, the recovery scheme can result in high concentrations of inorganics such as calcium, magnesium and sulfate. The latter might cause potential inhibition problems due to sulfate reduction to sulfide. The flowrate has increased from #*D*1 to #*D*2 from 144 $m^3.h^{-1}$ to 207 $m^3.h^{-1}$. An important difference between #*D*1 and #*D*2 is the addition of reject water to #*D*2, which originates from sludge stabilization of activated sludge. The latter contributes with a rather alkaline stream due to the use of lime (*CaO*) as stabilization agent during sludge treatment. It decreases the quantity of *NaOH* required for pH control at the same time as it supplies an extra source of COD in the form of particulate matter (total COD load 1600 kg $COD.h^{-1}$ in #*D*1 vs. 2200 kg $COD.h^{-1}$ in #*D*2).

A high frequency dynamic influent was generated based on the BSM2 influent generator (**Gernaey et al., 2011**)**.** The main idea behind this model is to assume specific (daily/weekly) industry-type defined profiles, which are sampled cyclically and combined by multiplication. The resulting output (averaged to 1) is scaled to the desired influent conditions assuming specific loading rates. Based on the available measurements, the BSM2 influent generator provides: 1) additional influent dynamics; 2) increased data frequency;

and, 3) a more realistic and complete picture of how the WTTP might perform under a wide range of disturbances **(Flores-Alsina et al., 2014; Snip et al., 2016**).

2.3. (Bio) chemical model

Reaction rates are evaluated using the stoichiometry and kinetics as described in the ADM1 (**Batstone et al., 2002a**). The operational temperature is constant at 35°C (mesophilic conditions). The default implementation is upgraded to include phosphorus (P), sulfur (S) and ethanol (Et-OH) related conversion processes as published in **Batstone et al. (2006), Soda et al. (2011) and Flores-Alsina et al. (2016)**. P is modelled using a source-sink approach assuming a predefined elemental (C, H, N, P, O) composition (**de Gracia et al., 2006**). Biological production of sulfides (S_{IS}) is described by means of sulfate reducing bacteria (X_{SRB}) utilising hydrogen (autolithotrophically) as electron source (**Batstone et al., 2006**). Potential hydrogen sulfide (Z_{H2S}) inhibition and stripping to the gas phase (G_{H2S}) is considered (**Fedorovich et al., 2003**). Finally, Et-OH ($S_{Et\text{-}OH}$) degradation is modelled assuming a specific group of microorganisms ($X_{Et\text{-}OH}$), which end up producing hydrogen (S_{H2}) and acetate (S_{ac}). Since the ΔG values and stoichiometry of hydrogen production are similar for ethanol and butyrate degraders, the default kinetic parameters and hydrogen inhibition parameters for butyrate degraders were used as starting values to describe ethanol degradation (**Batstone et al., 2004**). The model also includes physico-chemical equations that simulate the acid-base system and therefore pH (**Solon et al., 2015**). The model corrects for ionic strength via the Davies approach to consider chemical activities instead of molar concentrations, running all the calculations under non-ideal conditions (**Flores-Alsina et al., 2015**).

2.4. IC flow and reactor model

Figure 1 gives an overview of the proposed hydraulic configuration. *R1* (expanded sludge bed) and *R2* (polishing section) are modelled as a series of continuous stirred tank reactors (CSTR). *G–L* (gas-liquid separation) is modelled as a separate tank. High-rate conditions in the reactor are achieved by adding an ideal total suspended solids (TSS) separation unit (**Jeppsson et al., 2007**). As a result, it is possible to separate hydraulic residence time (HRT) and residence time of biomass (SRT). The latter is set to 100 days. The underflow is recirculated and combined back to *R1*, while the overflow with mainly soluble compounds leaves the reactor through the effluent. Finally, an additional external recirculation is included in the model as a combiner and a splitter system, in which the influent flow rate is set to the desired operational conditions. All model blocks have been implemented in the Matlab-Simulink software package (**Mathworks, Natick, MA, USA**).

2.5. Parameter estimation

Optimum values of kinetic coefficients for selected model parameters (**Table S4**) were estimated by separately fitting the dataset from each experiment, using a non-linear local optimization technique, lsqcurvefit in MATLAB, with the default 'trust-region-reflective' algorithm (Optimization Toolbox User's Guide Release 2014b, The MathWorks, Inc., Natick, MA, USA). Parameters to be estimated were based on literature (**Solon et al., 2013**) Biogas production values (CH_4, CO_2, H_2S) and process state variables (VFA, COD_{sol}, COD_{part}, COD_t, NH_x, $H_XPO_4^{3-X}$) were all selected and used as the fitted output being optimized (see **Table S4** for the specifics). The optimization was performed for one parameter and one output at a time. The residual sum of squares (RSS) was used as objective function. Further information about the method can be found elsewhere (**Lobry et al., 1991**).

2.6. Optimization scenarios

The model will be used to generate *response surfaces (RSs)* indicating optimal operational conditions. These *RSs* show the potential energy recovery from the IC reactor when operational conditions are modified. The operational settings tested were chosen based on the applicability, as only those that can practically be implemented in full-scale systems were taken into account. The optimization study is based on #*D*2. The following settings were tested.

1) Influent S (SO_4 and dissolved H_2S) versus operational pH. The pH in the plant is adjusted by chemical dosage. The S content of the influent can be modified by removing SO_4 prior to the anaerobic digester. There are currently ongoing studies to determine the best course of action for this process. One of the most economical ways to remove sulfate is through crystallization using calcium, producing gypsum (Tait et al., 2009). This method is most viable for waste streams containing more than 1 g S.L^{-1}, as sulfate and gypsum are in equilibrium at around 500 mg.L^{-1} (Silva et al., 2012). As the sulfate concentrations in this study are below 1 g S.L^{-1}, a more viable option would be adsorption on limestone (Silva et al., 2012). In a WWTP, removal of dissolved H_2S in the AD can be achieved by dosing iron salts in a tank prior to the AD reactor (Ge et al., 2013; Solon et al., 2017).

2) Influent pH and dissolved CO_2 (influent alkalinity). The content of inorganic carbon in the influent can be reduced by recycling part of the effluent stream into a smaller tank prior to the main anaerobic digester. The latter will promote CO_2 stripping to the gas phase causing an increase in pH (CO_2 has an acidic behaviour). This is common practice in P recovery systems, where stripping units are added to raise pH, which causes an increase of

PO_4^{3-} ions, which subsequently will lead to increased struvite crystallization (Jaffer et al., 2002).

2.7. Estimation of the energy recovery and reactor performance index

The estimation of the energy recovery is based on the amount of methane produced. It is assumed all the methane goes through a gas motor with 40 % efficiency for electricity and 50 % efficiency for heat. Electricity and heat prices are set to 0.15 €/kWh and 0.045 €/kWh, respectively **(AgroTech, 2014)**. The reactor performance index (RPI) **(Gernaey et al., 2014)** is used to evaluate the effects of the previously defined changes on the overall process performance. Specifically, the RPI accounts for: 1) the periodic purchase of chemicals for pH control; and, 2) methane production (and potential energy recovery). The cost of chemicals is based on the market price of NaOH (367 €/ton NaOH **(INTRATEC, 2017))**.

3. MODEL IMPLEMENTATION RESULTS

3.1. Mass balancing and influent fractionation

Influent characterization is based on elemental balancing following principles reported in **Nopens et al. (2009)**. Soluble inerts (S_I) (8 % in #*D*1 and 3 % #*D*2) are estimated from effluent COD_{sol}. It is assumed that 10 % and 78 % of the measured influent TSS concentration is inert material for #*D*1 and #*D*2, respectively, resulting in 6 % and 76 % X_I in COD_{part} for #*D*1 and #*D*2. This major difference in the inert material fraction is due to the addition of reject water in #*D*2, which containsa high fraction of inorganic material including precipitates. Amino acids (S_{aa}) and proteins (X_{pr}) are estimated using either soluble or particulate organic N forms and the N content of the aforementioned compounds. The ratio between $N_{organic,T}/NH_X$ and $N_{organic,S}/NH_X$ is twice as high for #*D*2 (4.0) as it is for #*D*1

(2.0), due to the addition of reject water (see dataset description in Section 2.2). The quantity of organic P is used to determine the fraction of lipids (X_{li}) based on the P content of lipids. Substantial $H_XPO_4^{3-X}$/$P_{organic,p}$ variation between #D1 and #D2 causes the differences in the P to COD ratio. In #D2 it is assumed that 44 % of the particulate P arrives as $P_{oganic,P}$, while the remaining 56 % are precipitates ($P_{inorganic,P}$). The remaining (non-acidified) COD_{sol} is allocated to fatty acids (S_{fa}). Since the influent wastewater is coming from the fermentation industry, sugars (S_{su}) and carbohydrates (X_{ch}) should only be present in low concentrations (consumed upstream). In fact, S_{su} and X_{ch} are assumed to be negligible due to a pre-acidification tank before the IC reactor. Volatile fatty acids (VFAs), inorganic carbon (S_{IC}), nitrogen (S_{IN}), phosphorus (S_{IP}) and sulfur (S_{SO4}, S_{IS}) values are obtained from measurements (see Section 2.2). A detailed graphical representation of the different COD fractions for the two data sets is depicted in **Figure 2.** Similarly to the influent, TSS, VFA, S_{IC}, S_{IN}, S_{IP} and sulfur (S_{SO4} and S_{IS}) values for the effluent are obtained from measurements.

Regarding conversion efficiencies, about 74 % of the total COD (COD_T) is converted to methane (CH_4) for #D1. The lower CH_4 production (60 %) achieved during the second evaluation period indicate substantial differences in the organics biodegradability, which is caused by the high X_I content of reject water added to #D2 (**Figure 2**). After digestion, most of the $N_{organic}$ is hydrolysed and therefore NH_X is increased up to 70 %. As there are no measurements of effluent particulate P, it was assumed the mass balance for P was maintained between the influent and effluent. The SO_X^{2-} reduction was between 50 and 60 % for both datasets, while the fraction SO_X^{2-}/H_XS^{2-X} was 0.8 for #D1 and 1.0 for #D2.

3.2. Model predictions versus full-scale data

The dynamic profiles of selected operational variables for the first evaluation period (#*D*1) are illustrated on the left side in **Figures 3 and 4** (dotted lines). Simulation results (solid lines) show that the proposed approach is capable to reasonably reproduce the process performance in terms of biogas production, COD conversion and nutrients transformations (N, P) (average deviations 13 % and 15 % for #*D*1 and #*D*2, respectively, see **Tables S2 and S3** for the specifics). The SO_4^{2-}, CH_4, CO_2 and H_2S profiles reveal the correct description of the mass transfer (liquid-gas), methanogenesis, sulfidogenesis and competition between methanogens (*MET*) and sulfate reducing bacteria (SRB). The model also predicts N (see NH_X profiles) and P (see $H_XPO_4^{3-X}$ profiles) release during anaerobic digestion processes from the hydrolysis of proteins and lipids. Parameter values were estimated by minimizing the sum of the squares of the deviation between the experimental results and the model predictions. The selection of these parameters was based on the Global Sensitivity Analysis results reported in **Solon *et al.* (2013)**.

Uptake rates for hydrogen degraders ($X_{H2,}$ $X_{SRB,H2}$) had to be adjusted in order to give a competitive advantage to SRB (**Batstone et al., 2006; Barrera et al., 2015**) (see Table S4). The slight accumulation of VFAs in the system was achieved by modifying two parameters. Firstly, K_s for acetate was increased in order to reduce the growth of specific biomass consuming acetate. Secondly, an additional inhibition factor was added to the VFA degraders, methanogens, SRB and ethanol degraders. This inhibition factor is directly multiplied with the corresponding K_s. The most probable reason for this addition is the potential inhibition on acetogens (X_{c4}, X_{pro} and X_{ac}) by an inorganic/organic compound neither measured nor described by the model. Finally, the content of C and N of S_I and biomass had to be adjusted in order to match CO_2, NH_x and $H_XPO_4^{3-X}$ profiles, as well as the P content of lipids and bacteria. All other parameters were left at their default values (Batstone et al., 2002a; Flores-Alsina et al., 2016). It is important to highlight that the addition of reject water during the second period (#*D*2) substantially changed influent biodegradability (see Figure 2). As a result it was necessary to adjust the P content of bacteria and lipids, as well as the N content of proteins. Furthermore, the K_s for acetate had to be reset to the default value (probably due to changing inhibition kinetics). All other parameter values were either default or the adjusted values found in #*D*1.

4. REACTOR OPTIMIZATION

4.1 Default operational conditions

For the current mode of operation (at a pH of 7.2), 135 MWh/d of electricity and heat is produced and 14 tons *NaOH*/d consumed, based on the model analysis. At an expected 320 production days per year and the economic numbers of section 2.7, this leads to an RPI of 1.96 M€/year. Hence, for the current mode of operation and expected 320 production days per year, the estimated RPI is 1.96 M€/year.

4.2 pH vs S

At the default operational pH, a lower influent S marginally increases methane production, and thus energy recovery (+ 5.7 %), reduces the use of chemicals (- 17.4 %) and finally increases the RPI (+ 24.6 %) (see Figure 5). This higher methane production is attributed to two factors: 1) competitive advantage to *MET* over *SRB* due to low influent S (Hao et al., 2014); and, 2) enhanced acidogenesis/acetogenesis due to less H_2S inhibition (Kalyuzhnyi and Fedorovich, 1998). There is also a lower dosing need of *NaOH* for pH control. Indeed, the reduction of S in the influent decreases the production of H_2S, a compound which acidifies the reactor in its dissolved form (HS^-). At the end of the year, this would lead to a RPI difference of 0.48 M€/year.

When the S load is not modified and the operational pH is decreased to 6.6, there is a slight reduction of methane production and energy recovery (- 1.3 %). On the other hand, there is a lower use of chemicals for pH control (less acidic conditions). In addition, it reduces the potential precipitation problems in the digester (currently not simulated in this version of the model, but commented upon in the discussion section) (Van Langerak et al., 2000; Latif et al., 2015). All in all, this would suggest an improvement with respect to the default situation of 1.96 M€/year (+ 63.5 %), resulting in an RPI of 3.20 M€/year. However, a pH of 6.6 is considered to be in the low range for anaerobic digestion, as the buffer capacity decreases at lower pH levels. From an operational point of view, a pH of 6.8 would therefore be more stable (Kroeker et al., 1979). This pH increases the RPI by 0.88 M€/year (+ 45.2 %). Combining these two strategies (removing the S from the influent and reducing the pH to 6.8), leads to a RPI of 3.31 M€/year (+69.2 %), an increase of 1.35 M€/year.

The results generated in this section clearly indicate that S does not impose any substantial reduction in process efficiency to warrant the potential cost for its removal, which is estimated to be approximately 3.58 M€/year. In the most optimistic case, S removal would lead to a 1.67 M€/year increase of the RPI. Calculation of S removal is based on the amount of limestone needed for the quantity of S in this case study (Silva et al., 2012) as well as an assumed market price of 0.085 €/kg limestone (Cree and Rutter, 2015). Interestingly, the additional simulation results depicted in Figure 6 reveal that the process could ensure similar methane production even at higher S loads as long as the operational pH is maintained above 6.8 (left plot in Figure 6). This is caused by the higher presence of H_2S (and decreased HS^-) increasing the S inhibition power on methanogens, VFA degraders, ethanol degraders and SRB. (pK_a of H_2S = 6.9). However, the cost for pH control would increase drastically in the event of a higher S load in the influent (middle plot in Figure 6). In this case a lower pH is more beneficial, as the dissolved H_2S is acidic and $NaOH$ is needed to increase the pH. The S loading can increase up to 2.5 times with a pH below 7.0 without exceeding the current need for $NaOH$. Combining these two effects into the RPI, the right plot in Figure 6 reveals that at a twofold increase of S, a decreased degree of performance compared to the current operational conditions can be expected from a pH of 7.0 and upwards (RPI falls below 1.96 M€/year).

4.3 CO_2 stripping

For the last scenario it was found that the higher the pH, the more impact CO_2 stripping has on the RPI (linear impact; right image in Figure 7). This is because the stripping of acidic CO_2 results in a loss of buffer capacity (Lisitsin et al., 2008), and it takes less caustic to reach a pH set point than in default conditions (no CO_2 recycling). At a pH of 7.2, which is the current operational pH, the RPI increases by 13.5 % (+ 0.62 M€/year) when CO_2 recycling is applied. However, in Section 4.2 it was recommended to operate at a pH of 6.8. At this pH an additional 6.8 % increase of the RPI (+ 0.19 M€/year) can be achieved on top of the previously determined 45.2 %.

5. DISCUSSION

This study presents a model-based approach to describe and optimize an anaerobic granular sludge internal recirculation (IC) reactor. First of all, a method based on COD, N, P and S mass balancing is used to determine the influent fractions. Secondly, it is detailed how to construct a flow + reactor model in order to reproduce high-rate conditions. The advantage of using two reactors as opposed to more is simulation speed. The more reactors you use, the slower the simulation time will become. On the other hand, more CSTRs will give a more stratified reactor (as in reality, where there is a gradient in biomass concentration from the bottom to the top). The simulation in two reactors was based on the IC reactor configuration, in which two main parts can be distinguished. A hydraulic CFD model will be needed to find how big the biomass gradient in fact is, and how important it is to model this as close to reality as possible. The resulting model was tested using two datasets. Results showed that the proposed approach was able to reproduce the reactor behaviour under different operational conditions (13 % and 15 % between plant measurements and model-based results). Finally, additional simulations were performed to find strategies to increase the energy recovery from the organics produced within the Novozymes and Novo Nordisk factories. It was found that decreasing the pH showed the highest potential in overall process performance. Hence, similar process performance could be achieved at lower pH and consequently increasing the RPI. It should be noted that the S loading to the reactor must not exceed a twofold increase compared to the current conditions when lowering the pH below 6.8 due to the formation of H_2S, which inhibits the methanogenic activity. On the other hand, the cost for *NaOH* addition increases substantially when the S loading is increased twofold and the pH is above 7.0. Under the current conditions the S loading does not limit the energy recovery such that it warrants removal. Furthermore, while stripping of CO_2 had no immediate impact on energy recovery, the loss of buffer capacity led to a decrease in *NaOH* addition, and thus an increase in RPI.

5.1 Economics

It is important to highlight that the RPI used in this case study provides an approximate idea of the potential running expenses for the reactor under study, but the entire picture is far from being complete. A proper energy balance should be carried out in order to have a more informed idea about potential recovery potential (Fernández-Arévalo et al., 2017). The costs derived from S are based on rough estimates found in literature (Cano et al., 2015; Cree and Rutter, 2015). The implementation of a new potential technology should be properly evaluated using rigorous metrics, such as net present value (NPV) and internal rate of return (IRR) (Gebrezgabher et al., 2010). These calculations should also capture uncertainty factors, such as the price of chemicals and operation, as well as unforeseen costs (Gargalo et al., 2016). Finally, the price of electricity and heat mentioned in Section 3.3 is assumed to be constant. However, energy prices can fluctuate on a daily basis and are location dependent (Weron, 2014). Aymerich et al. (2015) have shown that changing the energy consumption/production does not necessarily mean the energy costs or profits change. Still the authors believe that the results are valuable and can guide the process engineers in charge of running the plant to achieve better performance.

5.2 Opportunities

The presented methodology was applied for the optimization of energy recovery, by increasing the efficiency of the reactor performance. It was found that the largest increase in RPI (+ 45 %) could be obtained by decreasing the pH to 6.8. Another way to use the model is to find where the process is limited or where the limits of the process are, and thus determine its robustness. This study found that the evaluated bioreactor is robust to pH changes, which can be beneficial for control of the process, as well as to save costs on the addition of sodium hydroxide. It was also found that the presence of sulfur compounds does limit the methanogenic activity, but the highest impact was found for the *NaOH* dosing. When the concentration was increased up to twofold, the process had a higher dependency on *NaOH*, thus decreasing the RPI significantly (> 25 %).

5.3 Limitations

The model presented shows a good compromise between model complexity and predictive capabilities. While the average deviations are satisfactory, the model is not able to capture the dynamics of several components, as can be observed from the R^2 in Tables S2 and S3. This deficiency is most abundant in #*D*2 and most likely due to processes not considered in the model, such as inhibition by VFAs (Ahn et al., 2001), long chain fatty acids (Zonta et al., 2013) or compounds that were not measured. Furthermore, the proposed approach cannot describe the effect that (influent) inorganic material will have on process performance. Hence, high mineral content can lead to precipitation within the reactor. Precipitates will compete with bacteria for space in the reactor, again affecting the granular structure and the reactor performance (Van Langerak et al., 2000). These effects cannot be modelled with the current model, where an artificial loop is introduced to mimic the hydraulics of the reactor and the high biomass concentrations. This can, however, be done using a model based on a biofilm structure (Batstone et al., 2004; Feldman et al., 2017; Wanner et al., 2006). A biofilm model for the same system has been developed and yields similar results for the datasets available (Feldman et al., 2017). To simulate the effect of precipitation in the granules, special attention should be placed on defining a precipitation framework (Kazadi Mbamba et al., 2015) in order to determine saturation conditions. Furthermore, focus should be placed on density variation (Winkler et al., 2013), as well as the description of VSS and ISS concentrations in the granules (Ekama and Wentzel, 2004). The use of a biofilm model can indicate the long-term effect of intra-granular precipitation on methane production (Feldman et al., 2017, 2018).

6. CONCLUSIONS

The main findings of the presented study can be summarized in the following points:

- A mathematical model (ADM1 extended with physico-chemical, S and Et-OH reactions) has been developed and applied to an industrial anaerobic granular sludge internal circulation (IC) reactor. High loading conditions are reproduced using a flow + reactor model.
- Influent fractions are estimated using rigorous COD, N, P and S balances in order to characterize: 1) influent biodegradability; and, 2) the ratio between soluble and particulate compounds.
- The model has been adjusted using two datasets corresponding to different operational periods. A good resemblance between the experimental data and the model simulations indicates that the model is capable of describing hydrolysis, acidogenesis, acetogenesis, methanogenesis, sulfidogenesis, liquid-gas mass transfer and weak acid-base chemistry (13 % and 15 % of deviation for #*D*1 and #*D*2, respectively).
- Surface response plots were generated to demonstrate the potential of process optimization and increasing the energy recovery from the anaerobic digester. The optimization study shows that potential savings of 0.88 M€/year can be obtained simply by controlling the pH.

- Removing S from the influent does not yield enough energy to warrant the costs for its removal. However, at a twofold increase the drastic increase of *NaOH* addition reduces the RPI significantly at a pH of 7.0 and above. Furthermore, no significant effect could be obtained by stripping the CO_2 in a recycle loop for energy recovery, but it does lead to chemical cost savings (due to lower buffer capacity).

7. SOFTWARE AVAILABILITY

The Matlab-Simulink code of the model presented in this paper is available upon request. Using this code, interested readers will be able to reproduce the results summarized in this study. To express interest, please contact Prof. Krist V. Gernaey (kvg@kt.dtu.dk) or Dr. Xavier Flores-Alsina (xfa@kt.dtu.dk) at the Technical University of Denmark (Denmark).

8. ACKNOWLEDGMENTS

This work was done in collaboration with Novozymes A/S, Denmark. Financial support for the project from Novozymes A/S and the Technical University of Denmark is gratefully acknowledged. Dr Flores-Alsina gratefully acknowledges the financial support of the collaborative international consortium WATERJPI2015 WATINTECH of the Water Challenges for a Changing World Joint Programming Initiative (Water JPI) 2015 call as well as the GREENLOGIC ("Green chemical production using ecological control strategies") research project (DFF-FTP project 2, project no.: 7017-00175A). A concise version of this paper was presented at the 15th IWA World Conference on Anaerobic Digestion (Beijing, China, October, 2017) and the 8th International Young Water

Professionals Conference (Cape Town, South Africa, December, 2017). The authors declare that they have no conflict of interest.

9. NOMENCLATURE

ACP	Anaerobic contact processes
AD	Anaerobic digestion
ADM1	Anaerobic Digestion Model No. 1
AF	Anaerobic filters
AT	Anaerobic technologies
BSM2	Benchmark Simulation Model No. 2
CH_4	Methane production measurements ($m^3.day^{-1}$)
CSTR	Continuous stirred tank reactor
CO_2	Carbon dioxide production measurements ($m^3.day^{-1}$)
COD	Chemical oxygen demand
COD_t	Total chemical oxygen demand
COD_{part}	Particulate chemical oxygen demand
COD_{sol}	Soluble chemical oxygen demand
#*D*	Data set for model testing

EGSB	Expanded granular sludge bed
Et-OH	Ethanol
FB	Fluidized bed
G – L	Gas liquid separation unit
G_{CH4}	Methane production rate predictions (gas) (ADM1) ($m^3.day^{-1}$)
G_{CO2}	Carbon dioxide production rate predictions (gas) (ADM1) ($m^3.day^{-1}$)
G_{H2}	Hydrogen production rate predictions (gas) (ADM1) ($m^3.day^{-1}$)
G_{H2S}	Hydrogen sulfide production rate predictions (gas) (ADM1) ($kg.day^{-1}$)
H_2S	Sulfide production measurements ($m^3.day^{-1}$)
$H_XPO_4^{3-X}$	Phosphate measurements ($g.m^{-3}$)
H_XS^{2-X}	Sulfide (liquid) measurements ($g.m^{-3}$)
IC	Internal circulation
ISS	Inorganic suspended solids
N	Nitrogen
$N_{organic,S}$	Soluble organic nitrogen
$N_{organic,T}$	Total soluble nitrogen
NH_X	Ammonium/ammonia measurements ($g.m^{-3}$)

M	Mixing section
P	Phosphorus
PAT	Pre-acidification tank
pK_a	Acid dissociation constant
$R1$	Expanded sludge bed section of the reactor
$R2$	Polishing section of the reactor
RPI	Reactor performance index
RSs	Response surfaces
S	Sulfur
SI	Saturation Index
SO_X^{2-}	Sulfate/sulfite measurements (g.m^{-3})
SRB	Sulfate reducing bacteria
S_{aa}	Amino acids (ADM1) (kg COD.m^{-3})
S_{ac}	Total acetic acid (ADM1) (kg COD.m^{-3})
$S_{Biomass}$	S content in biomass (ADM1) (kmol S.kg COD.m^{-3})
S_{bu}	Total butyric acid (ADM1) (kg COD.m^{-3})
S_{Ca}	Calcium (ADM1) (kmol.m^{-3})

S_{Cl}	Chloride (ADM1) ($kmol.m^{-3}$)
$S_{Et\text{-}OH}$	Ethanol (ADM1) ($kmol.m^{-3}$)
S_{fa}	Fatty acids (ADM1) (kg $COD.m^{-3}$)
S_{H2}	Hydrogen (ADM1) (kg $COD.m^{-3}$)
S_{IC}	Inorganic carbon (ADM1) ($kmol.m^{-3}$)
S_{IN}	Inorganic nitrogen (ADM1) ($kmol.m^{-3}$)
S_{IP}	Inorganic phosphorus (ADM1) ($kmol.m^{-3}$)
S_{IS}	Inorganic total sulfides (ADM1) (kg $COD.m^{-3}$)
S_{K}	Potassium (ADM1) ($kmol.m^{-3}$)
S_{Mg}	Magnesium (ADM1) ($kmol.m^{-3}$)
S_{Na}	Sodium (ADM1) ($g.m^{-3}$) ($kmol.m^{-3}$)
S_{Pro}	Total propionic acid (ADM1) (kg $COD.m^{-3}$)
S_{Prot}	Sulfur in proteins (ADM1) (kmol.kg COD^{-1})
S_{Su}	Sugars (ADM1) (kg $COD.m^{-3}$)
S_{SO4}	Sulfate (ADM1) ($kmol.m^{-3}$)
S_{Va}	Total valeric acid (ADM1) (kg $COD.m^{-3}$)
TKN	Total Kjeldahl nitrogen measurements ($g.m^{-3}$)

TN	Total nitrogen measurements ($g.m^{-3}$)
TP	Total phosphorus measurements ($g.m^{-3}$)
TSS	Total suspended solids measurements ($g.m^{-3}$)
UASB	Upflow anaerobic sludge blanket
VFA	Volatile fatty acids measurements ($g.m^{-3}$)
V_{gas}	Gas volume in the bioreactor
V_{liq}	Liquid volume in the bioreactor
WWTP	Wastewater treatment plant
X_{ac}	Acetate degraders (ADM1) (kg $COD.m^{-3}$)
$X_{BIOMASS}$	Total biomass (ADM1) (kg $COD.m^{-3}$)
X_{C4}	Butyrate and valerate degraders (ADM1) (kg $COD.m^{-3}$)
X_{ch}	Carbohydrates (ADM1) (kg $COD.m^{-3}$)
$X_{Et\text{-}OH}$	Ethanol degraders (ADM1) (kg $COD.m^{-3}$)
X_{i}	Inert particulate organics (ADM1) (kg $COD.m^{-3}$)
X_{li}	Lipids (ADM1) (kg $COD.m^{-3}$)
X_{pr}	Proteins (ADM1) (kg $COD.m^{-3}$)
X_{pro}	Propionate degraders (ADM1) (kg $COD.m^{-3}$)

X_{SRB}	Sulfate reducing bacteria (ADM1) (kg COD.m^{-3})

10. REFERENCES

AgroTech. (2014). Methane emission from Danish biogas plants – Economic impact of identified methane leakages. *Report.* Aarhus, Denmark. Kurt Hjort-Gregersen.

Ahn, Y.H., Min. K.S., Speece, R.E. (2001). Pre-acidification in anaerobic sludge bed process treating brewery wastewater. *Water Res.* **35**, 4267–4276. https://doi.org/10.1016/S0043-1354(01)00171-3

APHA. (2012). Standard methods for the examination of water and wasttewater. American Public Health Association, Washington DC, USA.

Astals, S., Esteban-Gutiérrez, M., Fernández-Arévalo, T., Aymerich, E., García-Heras, J.L., Mata-Alvarez, J. (2013). Anaerobic digestion of seven different sewage sludges: A biodegradability and modelling study. *Water Res.* **47**, 6033–6043. https://doi.org/10.1016/j.watres.2013.07.019

Aymerich, I., Rieger, L., Sobhani, R., Rosso, D., Corominas, L. (2015). The difference between energy consumption and energy cost: Modelling energy tariff structures for water resource recovery facilities. *Water Res.* **81**, 113–123. http://dx.doi.org/10.1016/j.watres.2015.04.033.

Barrera, E.L., Spanjers, H., Solon, K., Amerlinck, Y., Nopens, I., Dewulf, J. (2015). Modeling the anaerobic digestion of cane-molasses vinasse: Extension of the Anaerobic Digestion Model No. 1 (ADM1) with sulfate reduction for a very high strength and sulfate rich wastewater. *Water Res.* **71**, 42–54. http://dx.doi.org/10.1016/j.watres.2014.12.026.

Batstone, D.J., Keller, J., Steyer, J.P. (2006). A review of ADM1 extensions, applications, and analysis: 2002 – 2005. *Water Sci. Technol.* **54**(4), 1–10. http://dx.doi.org/10.2166/wst.2006.520

Batstone, D.J, Keller, J., Angelidaki, I., Kalyuzhnyi, S.V., Pavlostathis, S.G., Rozzi, A., Sanders, W.T.M., Siegrist, H., Vavilin, V.A. (2002a). The IWA Anaerobic Digestion Model No 1. *Water Sci. Technol.* **45**(10), 65–73.

Batstone, D.J., Keller, J., Blackall, L.L. (2004). The influence of substrate kinetics on the microbial community structure in granular anaerobic biomass. *Water Res.* **38**, 1390–1404. https://doi.org/10.1016/j.watres.2003.12.003

Batstone, D.J., Torrijos, M., Ruiz, C., Schmidt, J.E. (2002b). Use of an anaerobic sequencing batch reactor for parameter optimisation in modelling of anaerobic digestion. *Water Sci. Technol.* **50**(10), 295–304.

Batstone, D.J, Hernandez, J.L.A., Schmidt, J.E. (2005). Hydraulics of laboratory and full-scale upflow anaerobic sludge blanket (UASB) reactors. *Biotechnol. Bioeng.* **91**, 387–391. https://doi.org/10.1002/bit.20483

Batstone, D.J., Puyol, D., Flores-Alsina, X., Rodríguez, J. (2015). Mathematical modelling of anaerobic digestion processes: Applications and future needs. *Rev. Environ. Sci. Biotechnol.* **14**, 595–613.

Bolle, W.L., Van Breugel, J., van Eybergen, G.C., Kossen, N.W.F., van Gils, W. (1986). An integral dynamic model for the UASB reactor. *Biotechnol. Bioeng.* **11**, 1621–1636. https://doi.org/10.1002/bit.260281106

Boltz, J.P., Morgenroth, E., Sen, D. (2010). Mathematical modelling of biofilms and biofilm reactors for engineering design. *Water Sci. Technol.* **62**, 1821–1836. https://doi.org/10.2166/wst.2010.076

Brockmann, D., Caylet, A., Escudié, R., Steyer, J-P., Bernet, N. (2013). Biofilm model calibration and microbial diversity study using Monte Carlo simulations. *Biotechnol. Bioeng.* **110**, 1323–32. https://doi.org/10.1002/bit.24818

Cano, R., Pérez-Elvira, S.I., Fdz-Polanco, F. (2015). Energy feasibility study of sludge pretreatments: A review. *Appl. Energy* **149**,176–185. http://dx.doi.org/10.1016/j.apenergy.2015.03.132.

Chen, Y., Cheng, J.J., Creamer, KS. (2008). Inhibition of anaerobic digestion process: A review. *Bioresour. Technol.* **99**, 4044–4064. https://doi.org/10.1016/j.biortech.2007.01.057

Chen, Z., Hu, D., Zhang, Z., Ren, N., Zhu, H. (2009). Modeling of two-phase anaerobic process treating traditional Chinese medicine wastewater with the IWA Anaerobic Digestion Model No. 1. *Bioresour. Technol.* **100**, 4623–4631. http://dx.doi.org/10.1016/j.biortech.2009.04.066.

Cree, D., Rutter, A. (2015). Sustainable bio-inspired limestone eggshell powder for potential industrialized applications. *ACS Sustain. Chem. Eng.* **3**, 941–949. http://dx.doi.org/10.1021/acssuschemeng.5b00035

Ekama, G.A., Wentzel, M.C. (2004). A predictive model for the reactor inorganic suspended solids concentration in activated sludge systems. *Water Res.* **38**, 4093–4106. https://doi.org/10.1016/j.watres.2004.08.005

Fang, H.H.P, Liu, H. (2002). Effect of pH on hydrogen production from glucose by a mixed culture. *Bioresour. Technol.* **82**, 87–93. https://doi.org/10.1016/S0960-8524(01)00110-9

Fedorovich, V., Lens, P., Kalyuzhnyi, S. (2003). Extension of Anaerobic Digestion Model No. 1 with processes of sulfate reduction. *Appl. Biochem. Biotechnol.* **109**, 33–45.

Feldman, H., Flores-Alsina, X., Ramin, P., Kjellberg, K., Jeppsson, U., Batstone, D.J., Gernaey, K.V. (2017). Modelling an industrial anerobic granular reactor using a multi-scale approach. *Water Res.* **126**, 488-500. https://doi.org/10.1016/j.watres.2017.09.033

Feldman, H., Flores-Alsina, X., Ramin, P., Kjellberg, K., Batstone, D.J, Jeppsson, U., Gernaey, K.V. (2018). Predicting the effects of intra-granule $CaCO_3$ precipitation in a full-scale industrial anaerobic biofilm reactor. *IWA Biofilms: Granular sludge conference*. Delft, The Netherlands, 18-21 March 2018.

Fernández-Arévalo, T., Lizarralde, I., Fdz-Polanco, F., Pérez-Elvira, S.I., Garrido, J.M., Puig, S., Poch, M., Grau, P., Ayesa, E. (2017). Quantitative assessment of energy and resource recovery in wastewater treatment plants based on plant-wide simulations. *Water Res.* **118**, 272–288. https://doi.org/10.1016/j.watres.2017.04.001

Flores-Alsina, X., Kazadi Mbamba, C., Solon, K., Vrecko, D., Tait, S., Batstone, D.J., Jeppsson, U., Gernaey, K.V. (2015). A plant-wide aqueous phase chemistry module describing pH variations and ion speciation/pairing in wastewater treatment process models. *Water Res.* **85**, 255–265. http://dx.doi.org/10.1016/j.watres.2015.07.014.

Flores-Alsina, X., Solon, K., Kazadi Mbamba, C., Tait, S., Gernaey, K.V., Jeppsson, U., Batstone, D.J. (2016). Modelling phosphorus (P), sulfur (S) and iron (Fe) interactions for dynamic simulations of anaerobic digestion processes. *Water Res.* **95**, 370–382. http://dx.doi.org/10.1016/j.watres.2016.03.012.

Flores-Alsina, X., Saagi, R., Lindblom, E., Thirsing, C., Thornberg, D., Gernaey, K.V., Jeppsson, U. (2014). Calibration and validation of a phenomenological influent pollutant disturbance scenario generator using full-scale data. *Water Res.* **51**, 172–185. https://doi.org/10.1016/j.watres.2013.10.022

Gargalo, C.L., Cheali, P., Posada, J.A., Gernaey, K.V., Sin, G. (2016). Economic risk assessment of early stage designs for glycerol valorization in biorefinery concepts. *Industrial & Engineering Chemistry Res*. **55**, 6801-6814. https://doi.org/10.1021/acs.iecr.5b04593

Ge, H., Zhang, L., Batstone, D.J., Keller, J., Yuan, Z. (2013). Impact of iron salt dosage to sewers on downstream anaerobic sludge digesters: Sulfide control and methane production. *J. Environ. Eng.* **139**, 594-601. https://doi.org/10.1061/(ASCE)EE.1943-7870.0000650

Gebrezgabher, S.A., Meuwissen, M.P.M., Prins, B.A.M., Oude Lansink, A.G.J.M. (2010). Economic analysis of anaerobic digestion – A case of Green power biogas plant in the Netherlands. *NJAS - Wageningen J. Life Sci.* **57**(2), 109–115. http://dx.doi.org/10.1016/j.njas.2009.07.006.

Gernaey, K.V., Jeppssson, U., Vanrolleghem, P.A., Copp, J.B. (2014). Benchmarking of control strategies for wastewater treatment plants. *IWA Sci. Tech. Rep. No. 23*. IWA Publishing, London, UK.

Gernaey, K.V., Flores-Alsina, X., Rosen, C., Benedetti, L., Jeppsson, U. (2011). Dynamic influent pollutant disturbance scenario generation using a phenomenological modelling approach. *Environ. Model. Softw.* **26**, 1255–1267. http://dx.doi.org/10.1016/j.envsoft.2011.06.001.

de Gracia, M., Sancho, L., García-Heras, J.L., Vanrolleghem, P.A., Ayesa, E. (2006). Mass and charge conservation check in dynamic models: Application to the new ADM1 model. *Water Sci. Technol.* **53**, 225–240. http://dx.doi.org/10.2166/wst.2006.025

Hao, T.W., Xiang, P.Y., Mackey, H.R., Chi, K., Lu, H., Chui, H.K., van Loosdrecht, M.C.M., Chen, G.H. (2014). A review of biological sulfate conversions in wastewater treatment. *Water Res.* **65**, 1–21. http://dx.doi.org/10.1016/j.watres.2014.06.043.

INTRATEC. (2017). Caustic Soda Price History. https://www.intratec.us/chemical-markets/caustic-soda-prices. Page accessed: 2 August 2017.

Jaffer, Y., Clarck, T.A., Pearce, P., Parsons, S.A. (2002). Potential phosphorus recovery by struvite formation. *Water Res.* **36**, 1834-1842. https://doi.org/10.1016/S0043-1354(01)00391-8

Jeppsson, U., Pons, M-N., Nopens, I., Alex, J., Copp, J.B., Gernaey, K.V., Rosen, C., Steyer, J-P., Vanrolleghem, P.A. (2007). Benchmark Simulation Model No. 2: General protocol and exploratory case studies. *Water Sci. Technol.* **56**(8), 67-78. http://wst.iwaponline.com/cgi/doi/10.2166/wst.2007.604.

Kalyuzhnyi, S.V., Fedorovich, V.V. (1998). Mathematical modelling of competition between sulphate reduction and methanogenesis in anaerobic reactors. *Bioresour. Technol.* **65**, 227–242. https://doi.org/10.1016/S0960-8524(98)00019-4

Kazadi Mbamba, C., Tait, S., Flores-Alsina, X., Batstone, D.J. (2015). A systematic study of multiple minerals precipitation modelling in wastewater treatment. *Water Res.* **85**, 359–370. http://dx.doi.org/10.1016/j.watres.2015.08.041.

Kroeker, E.J., Schulte, D.D., Sparlin, A.B., Lap, H.M. (1979). Anaerobic treatment process stability. *Water Pollution Control Federation* **4**, 718-727.

Van Langerak, E.P.A., Gonzalez-Gil, G., van Aelst, A., van Lier, J.B., Hamelers, H.V.M., Lettinga, G. (1998). Effects of high calcium concentrations on the development of methanogenic sludge in upflow anaerobic sludge bed (UASB) reactors. *Water Res.* **32**, 1255–1263. http://www.sciencedirect.com/science/article/pii/S0043135497003357.

Van Langerak, E.P.A., Ramaekers, H., Wiechers, J., Veeken, A.H.M., Hamelers, H.V.M., Lettinga, G. (2000). Impact of location of $CaCO_3$ precipitation on the development of intact anaerobic sludge. *Water Res.* **34**, 437–446. https://doi.org/10.1016/S0043-1354(99)00154-2

Latif, M.A., Mehta, C.M., Batstone, D.J. (2015). Low pH anaerobic digestion of waste activated sludge for enhanced phosphorous release. *Water Res.* **81**, 288–293. http://dx.doi.org/10.1016/j.watres.2015.05.062.

Van Lier, J.B., van der Zee, F.P., Frijters, C.T.M.J., Ersahin, M.E. (2015). Celebrating 40 years anaerobic sludge bed reactors for industrial wastewater treatment. *Rev. Environ. Sci. Biotechnol.* **14**, 681–702. http://dx.doi.org/10.1007/s11157-015-9375-5.

Lisitsin, D., Hasson, D., Semiat, R. (2008). The potential of CO_2 stripping for pretreating brackish and wastewater desalination feeds. *Desalination* **222**, 50-58. https://doi.org/10.1016/j.desal.2007.02.063

Lobry, J.R., Rosso, L., Flandrois, J.P. (1991). A FORTRAN subroutine for the determination of parameter confidence limits in non-linear models. *BINARY* **3**(86–93), 25.

Metcalf & Eddy, Burton, F.L., Stensel, H.D., Tchobanoglous, G. (2003). Wastewater engineering: Treatment and reuse. McGraw Hill, New York, NY, USA.

Nopens, I., Batstone, D.J., Copp, J.B., Jeppsson, U., Volcke, E., Alex, J., Vanrolleghem, P.A. (2009). An ASM/ADM model interface for dynamic plant-wide simulation. *Water Res.* **43**, 1913–1923. http://dx.doi.org/10.1016/j.watres.2009.01.012.

Odriozola, M., López, I., Borzacconi, L. (2016). Modeling granule development and reactor performance on anaerobic granular sludge reactors. *J. Environ. Chem. Eng.* **4**, 1615–1628. http://dx.doi.org/10.1016/j.jece.2016.01.040.

Punal, A., Trevisan, M., Rozzi, A., Lema, JM. (2000). Technical note influence of C:N ratio on the start-up of up-flow anaerobic filter reactors. *Water Res.* **34**, 2614–2619. https://doi.org/10.1016/S0043-1354(00)00161-5

Ren, T.T., Mu, Y., Ni, B.J., Yu, H. (2009). Hydrodynamics of upflow anaerobic sludge blanket reactors. *Environ. Energy Eng.* **55**, 516–528. https://doi.org/10.1002/aic.11667

Rieger, L., Takács, I., Siegrist, H. (2012). Improving nutrient removal while reducing energy use at three Swiss WWTPs using advanced control. *Water Environment Research*. **14**, 637-681. https://doi.org/10.2175/106143011X13233670703684

Saravanan, V., Sreekrishnan, TR. (2006). Modelling anaerobic biofilm reactors – A review. *J. Environ. Manage.* **81**, 1–18. https://doi.org/10.1016/j.jenvman.2005.10.002

Silva, A.M., Lima, R.M.F., Leão, V.A. (2012). Mine water treatment with limestone for sulfate removal. *J. Hazard. Mater.* **221-222**, 45–55. http://dx.doi.org/10.1016/j.jhazmat.2012.03.066.

Sipma, J., Osuna, M.B., Emanuelsson, M.A.E., Castro, P.M.L. (2010). Biotreatment of industrial wastewaters under transient-state conditions: Process stability with fluctuations of organic load, substrates, toxicants, and environmental parameters. *Crit. Rev. Environ. Sci. Technol.* **40**, 147–197. https://doi.org/10.1080/10643380802039329

Snip, L.J.P., Flores-Alsina, X., Aymerich, I., Rodríguez-Mozaz, S., Barceló, D., Plósz, B.G., Corominas, L., Rodriguez-Roda, I., Jeppsson, U., Gernaey, K.V. (2016). Generation of synthetic influent data to perform (micro)pollutant wastewater treatment modelling studies. *Sci. Total Environ.* **569-570**, 278–290. http://dx.doi.org/10.1016/j.scitotenv.2016.05.012.

Soda, S., Wada, K., Okuda, M., Ike, M. (2011). Application of modified ADM1 to long-term experiments for methane/hydrogen production from model organic waste. *Water Pract. Technol.* **6**(1), wpt2011009. http://dx.doi.org/10.2166/wpt.2011.009

Solon, K., Flores-Alsina, X., Gernaey, K.V., Jeppsson, U. (2013). Effects of influent fractionation, kinetics & stoichiometry and mass transfer on CO_2, CH_4 and H_2 production for (plant-wide) modelling of anaerobic digesters. In: *13th World Congr. Anaerob. Dig. Recover. Resour. World*. Santiago de Compostela, Spain, June 25-28 2013.

Solon, K., Flores-Alsina, X., Kazadi Mbamba, C., Volcke, E.I.P., Tait, S., Batstone, D., Gernaey, K.V., Jeppsson, U. (2015). Effects of ionic strength and ion pairing on (plant-wide) modelling of anaerobic digestion. *Water Res.* **70**, 235–245. http://dx.doi.org/10.1016/j.watres.2014.11.035.

Solon, K., Flores-Alsina, X., Kazadi Mbamba, C., Ikumi, D., Volcke, E.I.P., Vaneeckhaute, C., Ekama, G., Vanrolleghem, P.A., Batstone, D.J., Gernaey, K.V., Jeppsson, U. (2017). Plant-wide modelling of phosphorus transformations in wastewater treatment systems: Impacts of ontrol and operational strategies. *Water Res*. **113**, 97-110. https://doi.org/10.1016/j.watres.2017.02.007

Tait, S., Clarke, W.P., Keller, J., Batstone, D.J. (2009). Removal of sulfate from high-strength wastewater by crystallisation. *Water Res.* **43**,762–772. http://dx.doi.org/10.1016/j.watres.2008.11.008.

Vanhooren, H., Van Hulle, S.W.H., De Pauw, D.J., Vanrolleghem, P.A. (2002). Monitoring and modelling a pilot-scale trickling filter using on-line off-gas analysis. *Proc. Int. Spec. Conf. Biofilm Monit*. Porto, March. 2002. P. 17-20

Wanner, O., Eberl, H.J., Morgenroth, E., Noguera, D.R., Picioreanu, C., Rittmann, BE., van Loosdrecht, M.C.M. (2006). Mathematical modeling of biofilms. *IWA Sci. Tech. Rep. No. 18.* IWA Publishing, London, UK.

Weron, R. (2014). Electricity price forecasting: A review of the state-of-the-art with a look into the future. *International Journal of Forecasting* **30**, 1030-1081. https://doi.org/10.1016/j.ijforecast.2014.08.008

Winkler, M.K.H., Kleerebezem, R., Strous, M., Chandran, K., van Loosdrecht, M.C.M. (2013). Factors influencing the density of aerobic granular sludge. *Appl. Microbiol. Biotechnol.* **97**, 7459–7468. https://doi.org/10.1007/s00253-012-4459-4

Xavier, J.B., Picioreanu, C., van Loosdrecht, M.C.M. (2005). A framework for multidimensional modelling of activity and structure of multispecies biofilms. *Environ. Microbiol.* **7**, 1085–1103. https://doi.org/10.1111/j.1462-2920.2005.00787.x

Yun, Y.M., Sung, S., Shin, H.S., Han, J.I., Kim, H.W., Kim, D.H. (2017). Producing desulfurized biogas through removal of sulfate in the first-stage of a two-stage anaerobic digestion. *Biotech. Bioeng.* **114**, 970-979. https://doi.org/ 10.1002/bit.26233

Zonta, Ž., Alves, M.M, Flotats, X., Palatsi, J. (2013). Modelling inhibitory effects of long chain fatty acids in the anaerobic digestion process. *Water research*. **47**, 1369-1380. https://doi.org/10.1016/j.watres.2012.12.007

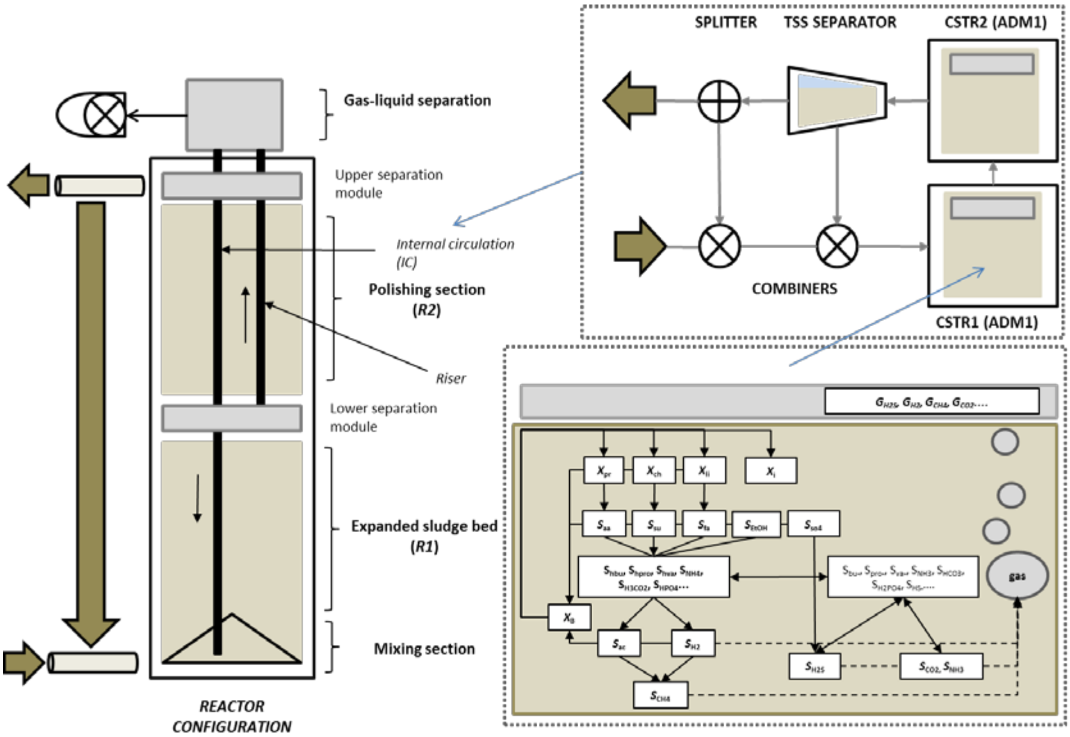

Figure 1. Schematic representation of the industrial reactor under study (left), the hydraulic model (top-right) and the main processes/states considered by the biochemical model (bottom-right).

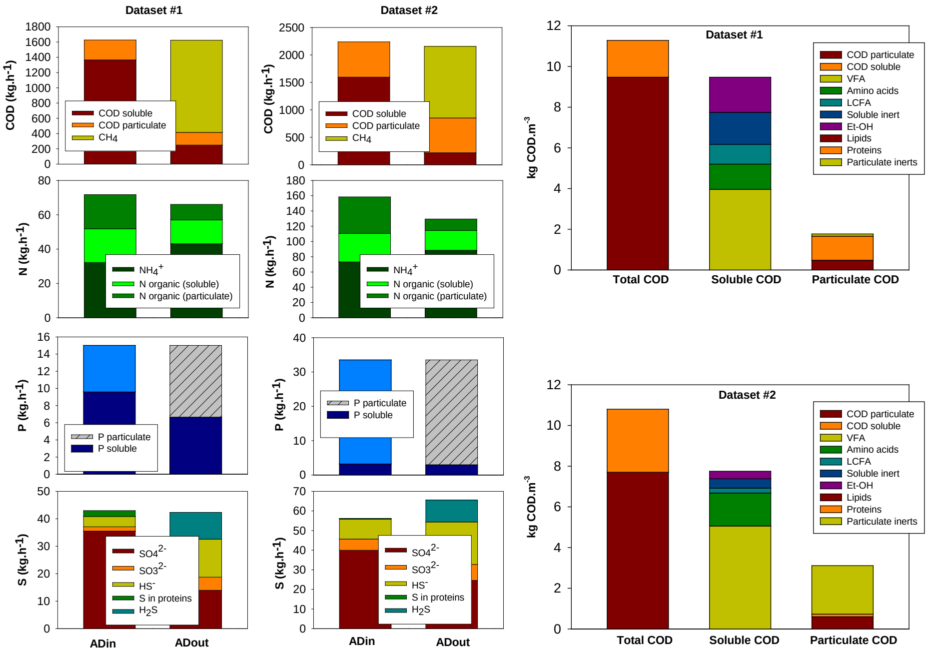

Figure 2. Mass balances for COD, N, P and S (left) and influent fractionation (right) for dataset #1 and dataset #2. For the effluent P no measurements of particulate matter were available, so P conservation was assumed (indicated by the striped bar).

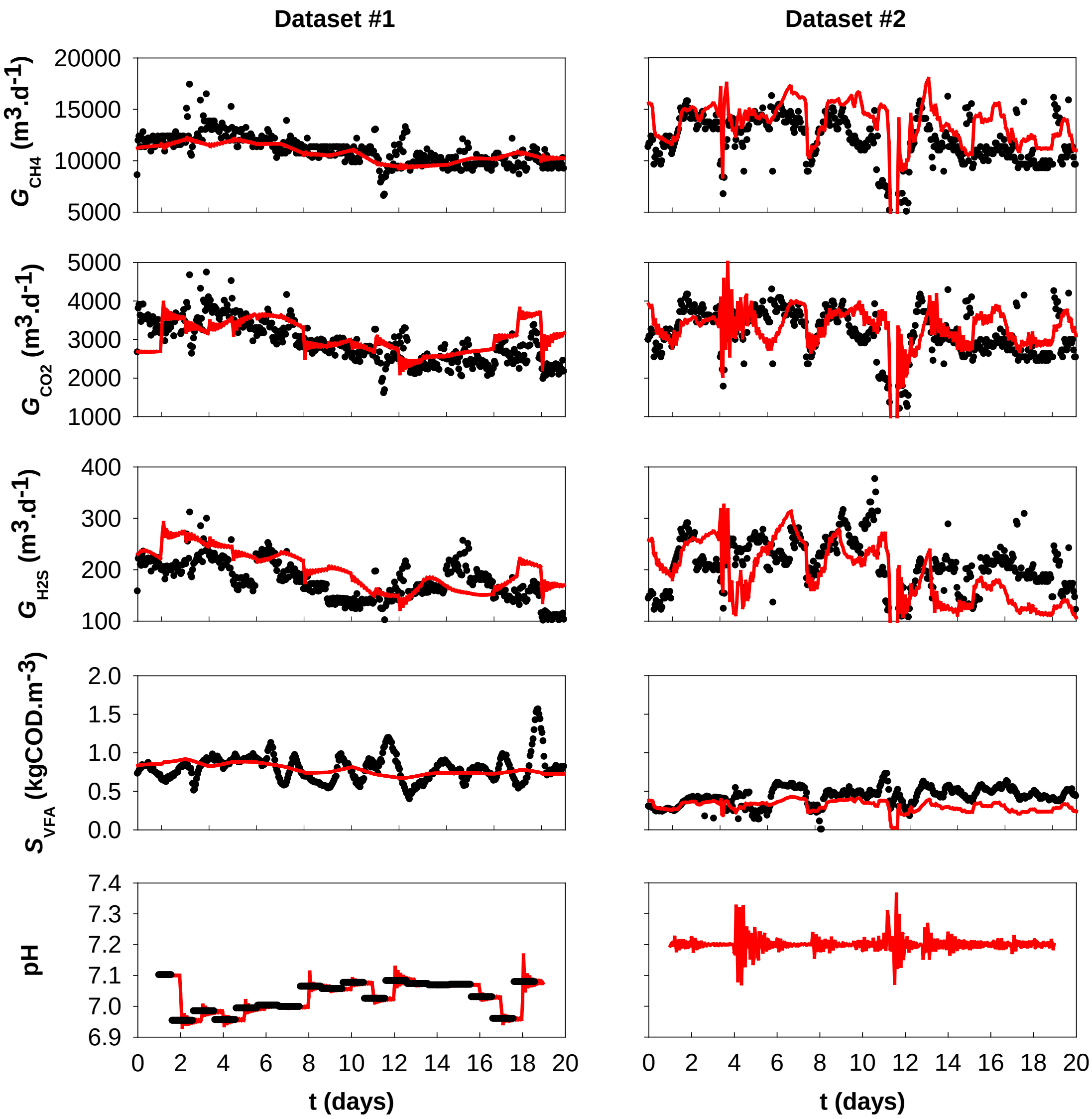

Figure 3. Simulated/on-line measurements for biogas (rows 1,2,3), VFA (row 4) and pH (row 5).

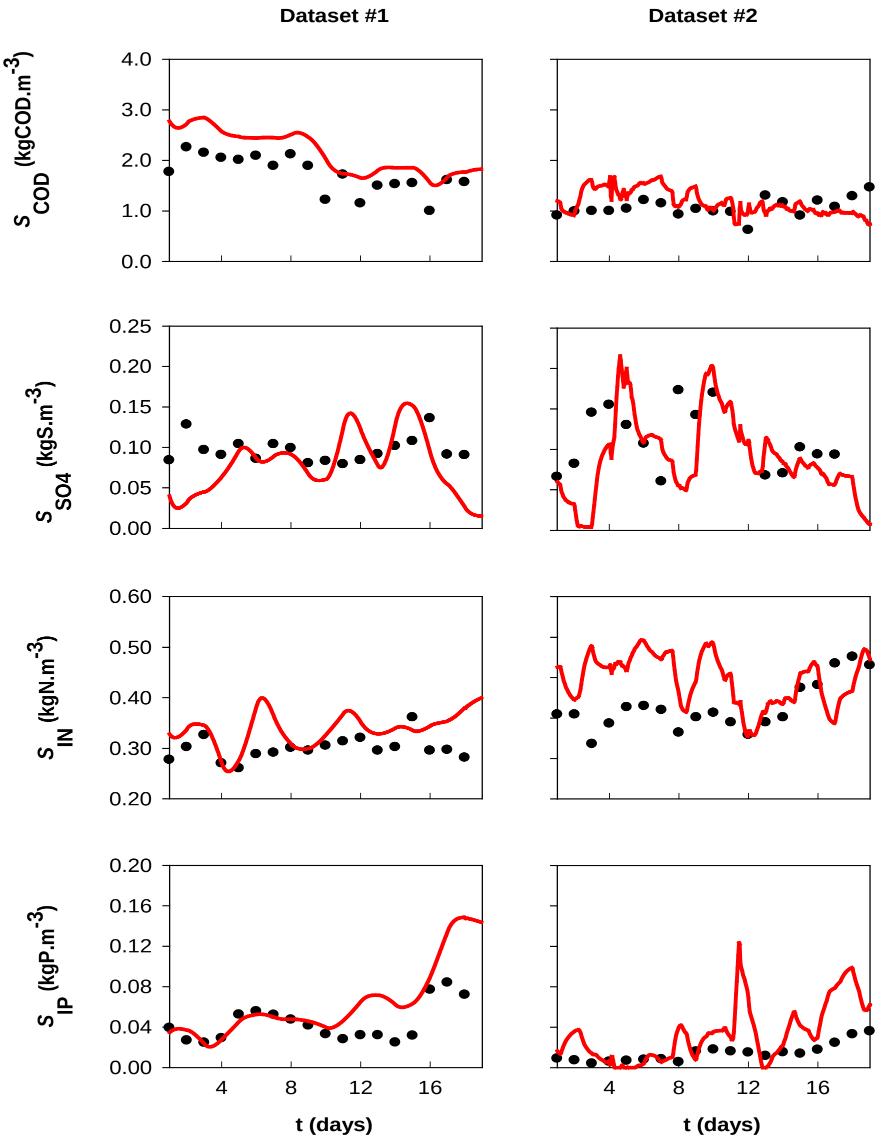

Figure 4. Simulated/off-line measurements for COD (row 1), SO_4 (row 2), NH_X (row 3) and $H_XPO_4^{3-X}$ (row 4).

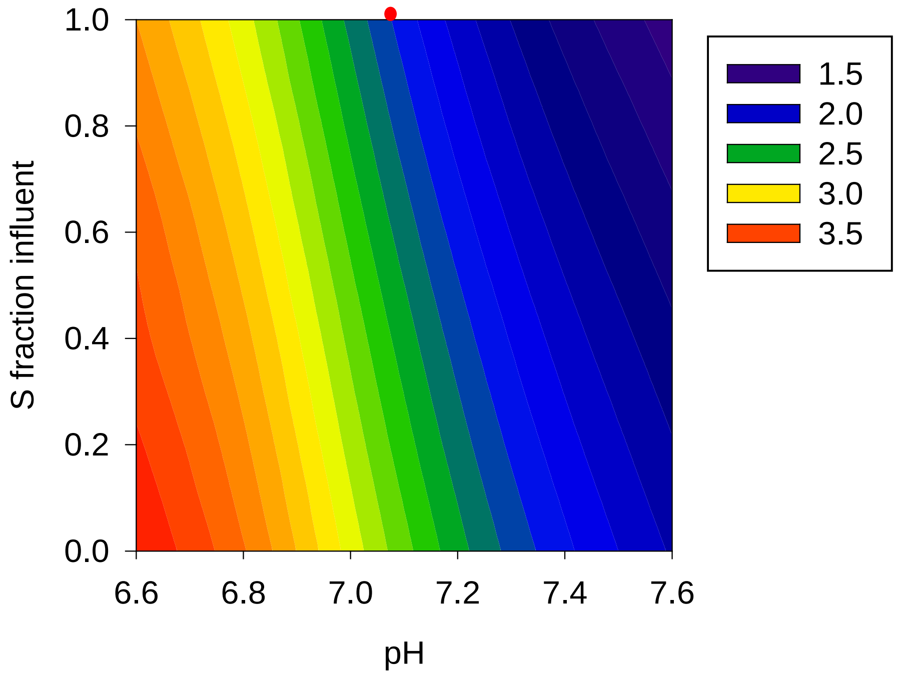

Figure 5. Response surfaces generated by changing: pH (x-axis) and sulfate and sulfide (y-axis). The simulations are based on #*D*2. The red dot represents current parameter settings. Results represent the RPI in M€/year.

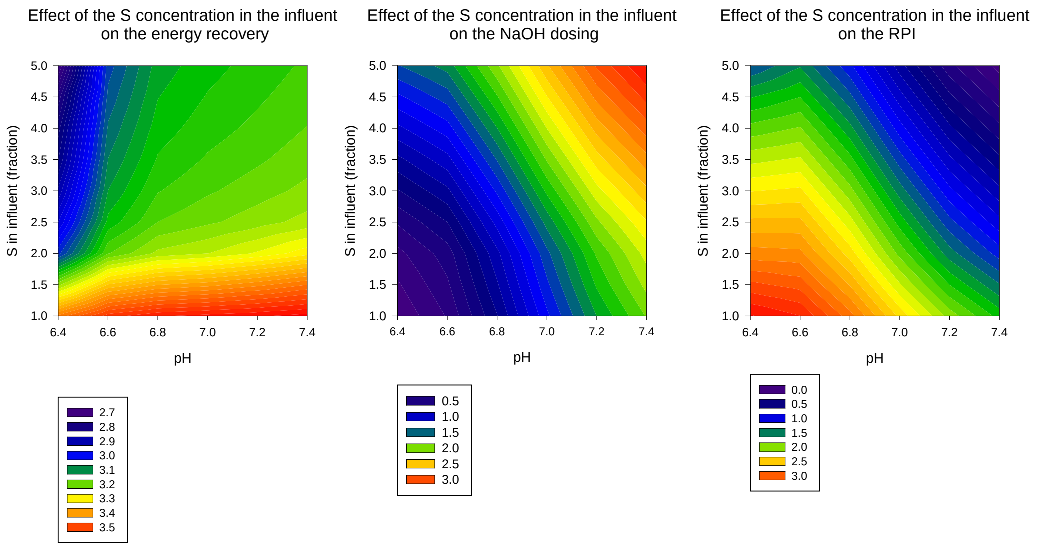

Figure 6. Response surfaces generated by changing the pH (x-axis) and sulfur compounds (y-axis) up to 5 times the current value in #*D*2. Left plot: RPI when only taking into account the energy recovery (M€/year); Middle plot: The cost of *NaOH* (M€/year); Right plot: The RPI when taking both the energy recovery and need of *NaOH* for pH control into account (M€/year).

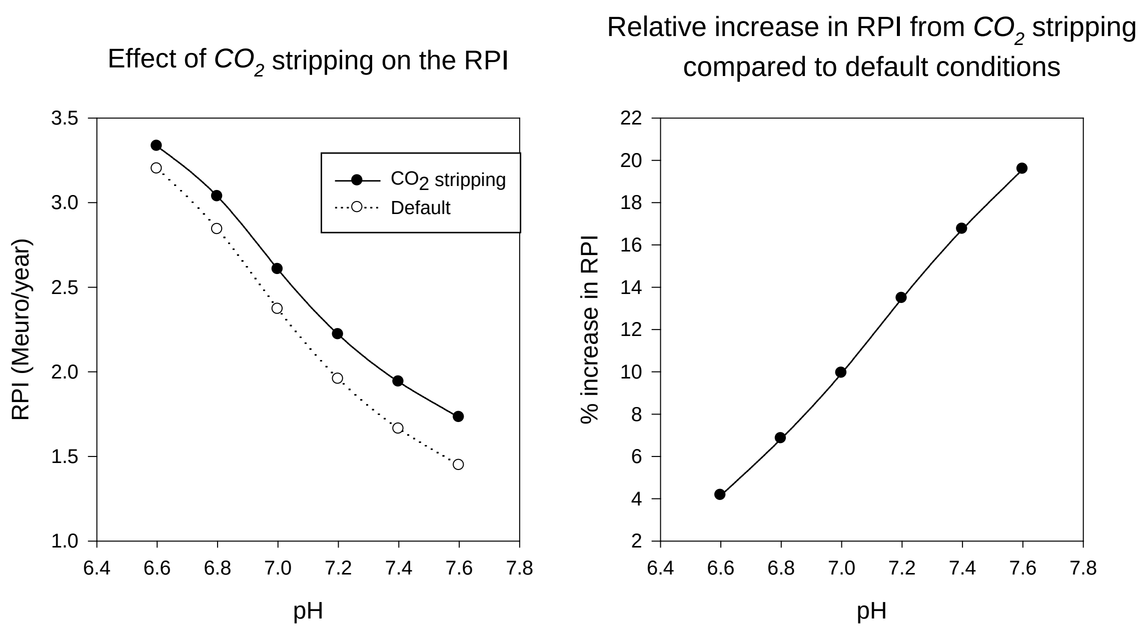

Figure 7. Effect of CO_2 stripping and the pH on the RPI (left) and the increase in RPI (%) compared to the case when CO_2 stripping is not applied (right).